ECI Symposium Series, Volume RP2: Proceedings of 6th International Conference on Heat Exchanger Fouling and Cleaning - Challenges and Opportunities, Editors Hans Müller-Steinhagen, M. Reza Malayeri, and A. Paul Watkinson, Engineering Conferences International, Kloster Irsee, Germany, June 5 - 10, 2005

PARTICULATE FOULING GROWTH RATE AS INFLUENCED BY THE CHANGE IN THE FOULING LAYER STRUCTURE

M.S. Abd-Elhady[1,*], C.C.M. Rindt[1], J.G. Wijers[2] and A.A. van Steenhoven[1]

[1] Department of Mechanical Engineering,
[2] Department of Chemical Engineering,
Eindhoven University of Technology, P.O. Box 513, 5600 MB Eindhoven, The Netherlands.
[*]Corresponding author, E-mail: m.s.abd-Elhady@tue.nl

ABSTRACT

Particulate fouling in biomass gasifiers is a major problem, which may lead to inefficient operation. As the fouling layer grows, its thermal resistance increases resulting in an increase in the surface temperature of the fouling layer. The increase in the fouling layer surface temperature can lead to sintering of the layer, which changes the layer structure from a fragile powder to a robust coherent structure. The influence of the change in the fouling layer structure on the growth rate of particulate fouling is studied experimentally. Impaction experiments were carried out to determine the velocities at which an incident particle sticks, bounces off or removes particles out of the fouling layer as a function of fouling layer structure. The sticking velocity of a particle hitting a clean tube is determined theoretically. The sticking velocity of a bronze particle hitting a bronze plate is 0.006 m/s, for a powdery layer is 0.3 m/s and for a sintered layer is 0.04 m/s. The change in the heat exchanger surface from solid to powdery increases the sticking velocity, which consequently speeds up the fouling process. The further change in the heat exchanger surface from powdery to sintered decreases the sticking velocity, which reduces back the fouling process. The change in the fouling layer structures affects the sticking velocity as well as the removal velocity of incident particles, which consequently affect the fouling process.

INTRODUCTION

During biomass gasification, particles (fly ashes) are entrained from the biomass into the flue gasses. These particles consist of refractory species, which are composed mainly of sulphates, chlorides (Bryers, 1996; Miles et al., 1996) and carbon, and their size can vary between few microns and some 100 μm. These contaminants deposit on the gas-cooler heat exchangers forming an insulating layer, which reduces the overall heat transfer coefficient and can result in operation failure. The accumulation of particles on a heat exchanger surface forming an insulating powdery layer is known as particulate fouling. The growth rate of particulate fouling layers is determined by the difference between the deposition and the removal rates of particles on and from the fouling layer (Kern and Seaton, 1959). The stages of particulate fouling are illustrated in fig. 1. The fouling layer thermal resistance R_f, expressed in [m^2K/W], is related to its thermal conductivity k and thickness δ by

$$R_f = \frac{\delta}{k}. \qquad (1)$$

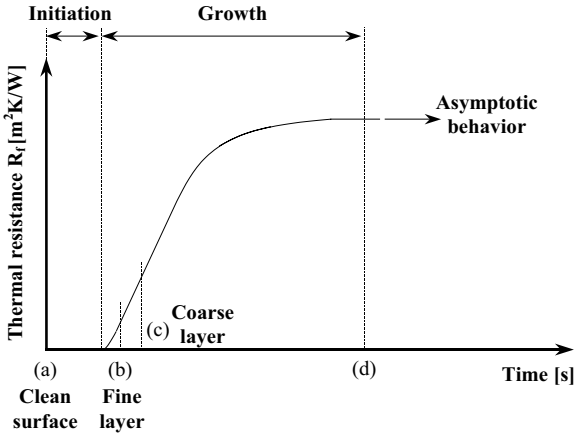

Fig. 1 Stages of particulate fouling.

At the beginning of operation (**a**), the heat exchanger tubes are clean and the fouling layer growth is slow. The initial deposit layer (**b**) is likely to be of fine particles, which are transported by the thermophoresis mechanism (Rosner, 1980; Wagoner and Yan, 1991). Due to the temperature gradient between the gasses and the heat exchanger surface, the particles in the flue gasses experience a force in the direction towards the cooler surface. This so-called thermophoretic effect augments the transport of sub- to micrometer particles towards the heat exchanger surface. The velocities with which the particles arrive at the surface due to thermophoresis are low, and, therefore most of them stick to the surface. Semi-empirical models for calculating the particle deposition rate based on thermophoresis were developed by Friedlander and Johnstone (1957), Cleaver and Yates (1975), Wood (1981), Papavergos and Hedley (1984) and Fan and Ahmadi (1993).

Most of these models do not take into account the effect of particle re-entrainment on the deposition rate. Thickening of the fine layer results in the collection of larger particles (**c**), which are transported mainly by inertial impaction (Israel and Rosner, 1983). As calculated by van Beek et al. (2001), the transportation rate by inertia is at least one order of magnitude larger than thermophoresis. This does not imply that transportation by impaction causes a higher fouling rate than thermophoresis. Particles that are transported by impaction hit the heat exchanger surface with a velocity larger than the one by thermophoresis, which can cause the particles to bounce off or even remove other particles from the fouling layer. The interaction between the incident particle and the deposit is an important issue for modeling the growth rate of particulate fouling and needs to be further studied.

As the coarse particulate layer continues to grow (**d**), the thermal resistance of the layer continues to increase. During the development of this particulate layer, the temperature difference over the deposit, and therefore the temperature of its surface, will continuously increase. As a result, the fouling layer sinters. Sintering leads to the reduction of the void volume and reinforcement of the contact bridges between particles (Ristic, 1979). The degree of sintering depends upon the gas side temperature and sintering time (Wall et al., 1993). At this stage (**d**) where sintering has already started, a steady state may develop during the deposit growth. This steady state of deposit growth is known as the asymptotic behavior of particulate fouling and it is shown by the horizontal arrow in fig. 1. The asymptotic behavior has been reported by many researchers in different applications; in a waste incinerator by van Beek et al. (2001), in a coal-fired power plant by Bott (1988) and in a biomass/coal co-firing power plant by Baxter (1993). The reason behind the asymptotic behavior is not confirmed. At a certain stage of fouling the removal rate of particles from the deposit balances the deposition rate and that could be due to an increase in the removal rate or a decrease in the deposition rate.

The objective of this research is to study the influence of the change in a heat exchanger surface during operation on the growth rate of particulate fouling layers. The incident velocities at which an incident particle sticks to the fouling layer, rebounds from the surface or removes particles from the fouling layer are important parameters in determining the growth rate of particulate fouling layers. Impaction experiments are carried out to determine the mentioned velocities for a powdery fouling layer and a sintered layer. The impaction experiments were carried out in a vacuumed column, where particles are dropped onto the prepared fouling layer at the bottom of the vacuumed column and the particles ejected due to impact were counted as a function of the impact speed. The model of Rogers and Reed (1984) was used to determine the sticking velocity for a particle hitting a clean tube. Based on the variation of the critical sticking and removal velocities as a function of the fouling layer structure conclusions are drawn about the influence of the fouling layer structure on the growth rate of particulate fouling layers.

IMPCTION EXPERIMENTS

Experimental setup and experimental procedure

An experimental set-up has been built to determine the impact speed at which an incident particle sticks, bounces off or removes particles out of a bed of particles. The set-up consists of a vacuumed column in which particles are released from a particle feeder onto a bed of particles. The particle feeder is installed in the top-segment of the column as shown in fig. 2.a. The vacuumed column is optically accessible by two windows. The trajectory of the particles is recorded using a digital camera system. A pulsated light sheet illuminates the particle several times in one camera image. For each particle, the impact velocity is determined from the average distance between two successive illuminations (blobs) and the rate of pulsation of the laser sheet. Further details about the measurement procedure and analysis can be found in van Beek (2001). At the bottom of the vacuumed column, a bed of particles was installed on a horizontal object table.

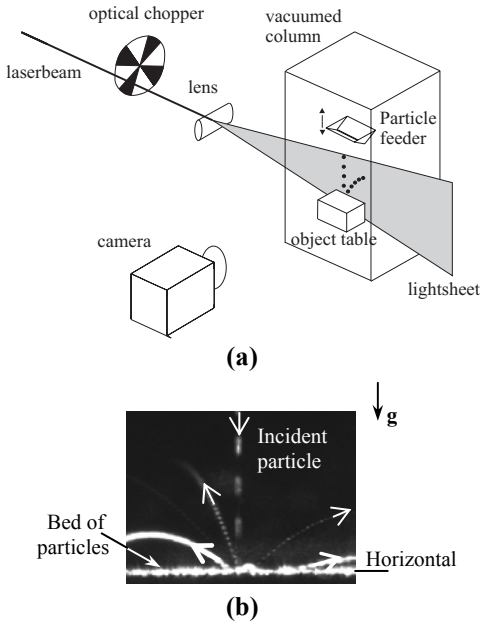

Fig. 2 The experimental set-up (a) and a typical recorded image (b) showing a particle falling vertically onto a bed of particles and ejecting particles out of the bed.

In the experiments particles similar to the bed particles were dropped vertically onto the bed and the particles ejected due to impact were counted. The incident particle impact speed, angle and rebound speed were measured. The vertical speed of the incident particle $V_{i,y}$ was varied from 0.01 to 3.5 m/s by varying the drop height (height of the vacuumed column). $V_{i,y}$ is the incident particle speed in the direction of gravity. A schematic of the experimental set-up and a typical recorded image of a particle falling vertically onto a bed of particles and ejecting particles out of the bed are shown in fig. 2.b.

Sample preparation and particles used

The particles used in the impaction experiments and the fouling layers preparation are spherical bronze particles of average diameter 54 μm with a standard deviation of ± 3 μm. The bronze particles were chosen to represent the soft fouling particles in biomass gasifiers that can easily deform under small colliding velocities, such as lead, carbon, zinc and magnesium (Brunner et al., 2002), which represent the majority of particles. The particle size distribution and a scanning electron microscope (SEM) image for the spherical bronze particles used, are shown in fig. 3. Two fouling layers are prepared by pouring the bronze particles in two sample holders of size 20 mm × 20 mm × 5 mm, and shaking them for 30 minutes to ensure that porosity is equally distributed in the layer. One sample holder is placed in a nitrogen tube oven for 20 hours at 500 °C to prepare a sintered fouling layer, the other sample holder represents a powdery fouling layer. A SEM image of the neck formed between two sintered particles in the 20-hour sample is shown in fig. 4. The degree of sintering is measured by the size of the neck formed, which is a function of the heating temperature and time (Frenkel, 1945; Kuczynski, 1949). The neck diameter X of the powdery sample is 0 μm and of the 20 hr-sample is 12 μm ± 1 μm. The neck diameter of the sintered layer was measured from the SEM images taken, where 20 particles were checked and the average diameter was calculated. The average degree of sintering X/D for the powdery layer is 0 and for the sintered layer is 0.22, where D is diameter of the particle before sintering.

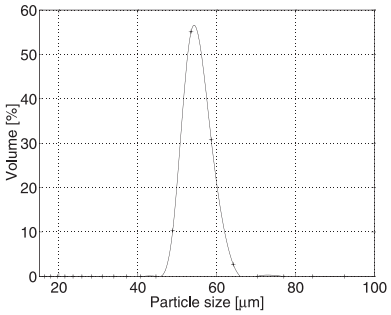

(a)

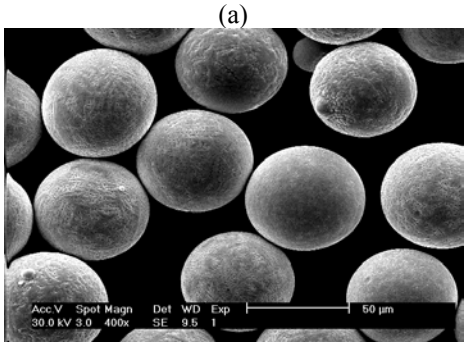

(b)

Fig. 3 (a) Particle size distribution of the bronze particles used in the impaction experiments. The Average diameter is 54 mm and the standard deviation is ± 3 μm. (b) A scanning electron microscope image of the bronze particles.

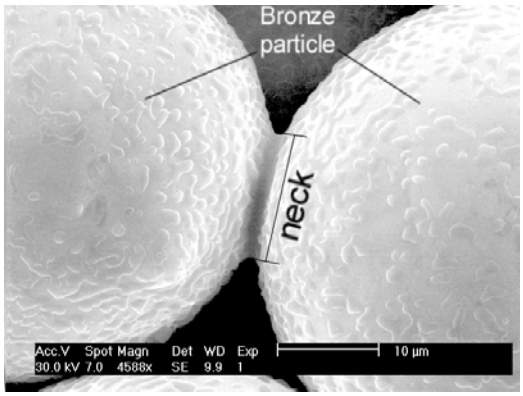

Fig. 4 Neck formed between two sintered bronze particles.

Experimental results

490 experiments were performed at different impact speeds. The experiments were categorized based on the particle post-collision behaviour. The experiment number and the corresponding vertical impact speed for a certain post-collision event, i.e. sticking, bouncing and removal are shown in fig. 5. As can be seen from fig. 5.a, 105 experiments have been performed at different impact speeds ranging from 0.01 m/s to 0.3 m/s and they all showed sticking of the incident particle to the bed. The average impact speed for sticking is 0.13 m/s with a standard deviation of 0.09 m/s. The bouncing off and the removal cases are shown in figs. 5.b and 5.c respectively. The average impact speed and standard deviations are respectively: 0.6 ± 0.22 m/s for bouncing and 1 ± 0.27 m/s for removal.

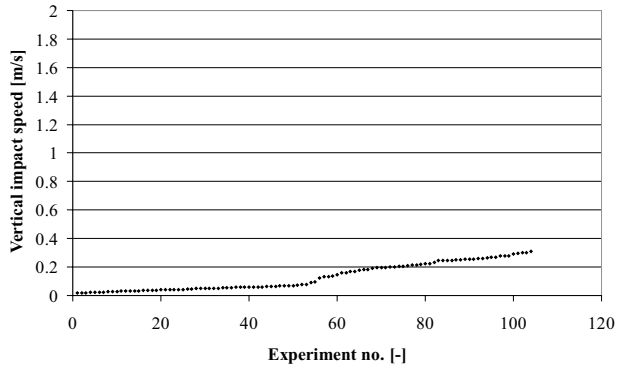

(a) Range of vertical impact speeds where the incident particle *sticks*.

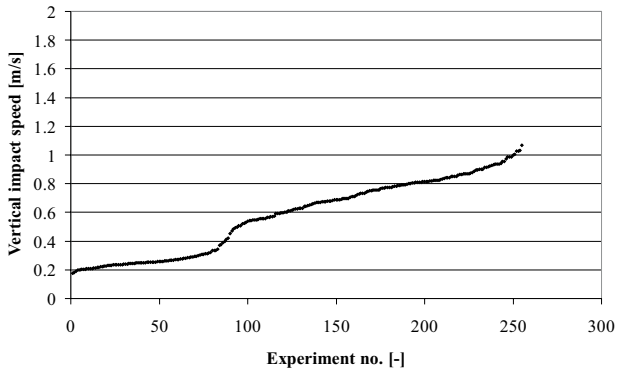

(b) Range of vertical impact speeds where the incident particle *rebounds*.

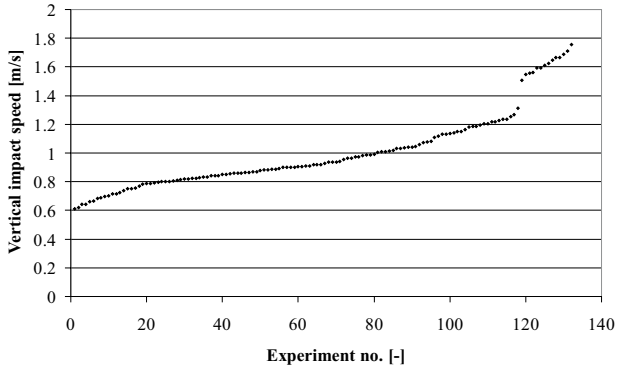

(c) Range of vertical impact speeds where the incident particle *rebounds and removes* one particle.

Fig. 5 The post-collision behaviour of the incident particle as a function of the vertical impact speed. particle (a) sticks, (b) bounces off and (c) rebounds and removes one particle out of the bed of particles. The x-axis represents the experiment number according to the sequence of the impact speed.

The results shown in fig. 5 are summarized in fig. 6.a in which the number of particles ejected from the prepared bed of particles as a function of the incident particle vertical speed is shown. Figures 5.a and 6.a show that the incident particle sticks to the bed of particles if the impact speed is below 0.3 m/s and bounces off the bed if the impact speed is between 0.18 and 1.1 m/s, see figs. 5.b and 6.a. The incident particle can bounce off and remove one particle or more from the bed if the impact speed is above 0.6 m/s. We only show the data for the removal of one particle in fig. 5.c. Above a velocity of 1.5 m/s two or more particles are removed, but due to the available experimental conditions only a limited amount of data is available. As can be seen from fig. 6.a, there are velocity regimes at which the incident particle sticks, bounces off or removes particles from the bed of particles. The overlapping in the number of particles ejected is due to the variation of the local impact angle (Abd-Elhady, 2005), i.e. the position where the incident particle hits the target particle, for the same vertical impact speed.

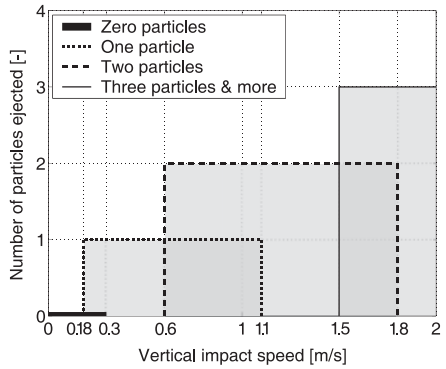

(a)

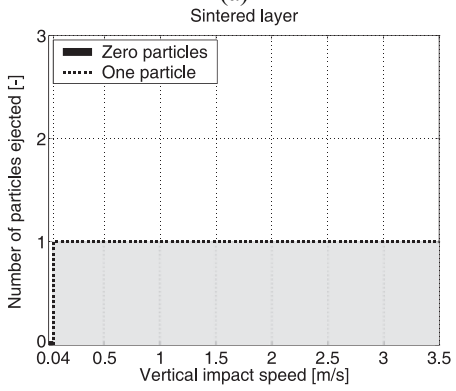

(b)

Fig. 6 Number of particles ejected from a powdery layer (a) and a sintered layer (b) due to an incident particle impact. The incident particle and the layer particles are of the same material, bronze and average diameter, 54 μm. The average degree of sintering X/D for the sintered layer is 0.22 and for the powdery layer is 0.

The results of the impaction experiments for the sintered layer are shown in fig. 6.b. The critical sticking velocity (CSV) is defined as the maximum impact speed at which an incident particle sticks to a bed of particles (Abd-Elhady et al., 2005). From the experiments it can be concluded that the critical sticking velocity for the sintered bronze layer is 0.04 m/s, which is 7.5 times lower than the sticking velocity for the powdery layer, 0.3 m/s. Sintering strengthens the bonding between the bed particles and therefore the particles in the sintered layer can only move as a whole, which consequently reduces the energy losses, due to an incident particle impact and therefore lowers the sticking velocity. The removal of a bed particle, due to an incident particle impact, is hardly to occur, due to the strong bonding between the sintered bed particles. An incident particle impact with an impact speed of 3.5 m/s had still not sufficient energy to remove a particle out of the layer, as have been seen from the experiments.

THE CSV FOR A PARTICLE HITTING A CLEAN HEAT EXCHANGER TUBE

The model of Rogers and Reed (1984) was used to determine the sticking velocity for a particle hitting a clean tube. The Rogers and Reed model describes the adhesion of a particle to a massive plate following an elastic-plastic impact based upon consideration of the energy losses during impact. The energy balance is as follows for a particle of mass m impacting normally a stationary massive plate with a velocity $V_{i,n}$

$$\frac{1}{2}mV_{i,n}^2 + Q_A = Q_e + Q_p, \qquad (2)$$

with the left hand side of the equation the energy at the beginning of the collision and the right hand side the energy at the end of the approach phase. Q_A is the adhesive energy due to the attractive forces between the incoming particle and the surface, Q_e is the stored elastic energy and Q_p is the energy loss due to plastic deformation. If the stored elastic energy Q_e is larger than the adhesive energy Q'_A required to separate the particle from the surface then the particle will rebound otherwise it will stick to the surface. The mentioned energy terms are calculated based on the concept of contact mechanics (Johnson, 1985; Thornton and Ning; 1998), and they are determined theoretically based on the physical properties of the interacting particles. The above energy terms are described in detail in (Rogers and Reed, 1984; van Beek, 2001).

$$\frac{1}{2}mV_{r,n}^2 = Q_e - Q'_A. \qquad (3)$$

The Rogers and Reed model was solved for bronze particles of diameter 54 μm hitting a massive bronze plate at different impact speeds and the results are depicted in fig. 7. The bronze particle represents the fouling particles in biomass gasifiers and the bronze plate represents the heat exchangers tubes. The physical properties of the bronze used in the calculations are shown in table 1. The relevant mechanical properties of bronze shown in table 1 were taken the same as those of copper. Figure 7 shows the variation of the coefficient of normal restitution, e_n, with the normal impact speed, $V_{i,n}$. The coefficient of restitution is defined as the ratio between the normal rebound speed, $V_{r,n}$, and the normal impact speed, $V_{i,n}$, for a particle hitting a massive plate. Figure 7 shows that if a bronze particle of diameter 54 μm hitting a bronze plate at a speed lower than 0.006 m/s it will stick, i.e. $V_{r,n} = 0$ and $e_n = 0$.

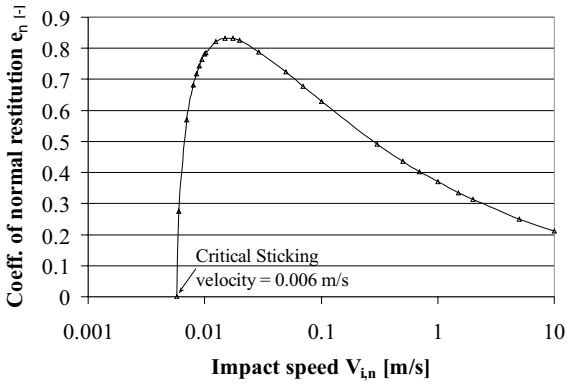

Fig. 7 Coefficient of normal restitution e_n for a bronze particle of diameter 54 μm hitting normally a mass bronze plate at different impact speeds $V_{i,n}$.

Table 1. Physical properties of bronze (Rogers and Reed, 1984).

	Bronze
Young's modulus, E (N/m^2)	1.29×10^{11}
Yield strength, y (N/m^2)	3×10^{8}
Density, ρ (kg/m^3)	8960
Poisson's ratio, ν	0.33
Surface energy, Γ (J/m^2), bronze - bronze	0.12

DISCUSSION OF RESULTS

The critical sticking velocity is plotted in fig. 8 for a bronze particle hitting fouling layers of different degrees of sintering X/D, where X is the diameter of the neck formed between the particles of the sintered layer and D is the diameter of the particles before sintering. The diameter of the bronze particles before sintering is 54 μm ± 3 μm. The critical sticking velocity at X/D=1 is the sticking velocity for a fully sintered layer, i.e. a solid plate, and it was calculated by the model of Rogers and Reed in the previous section. The critical sticking velocity at a zero degree of sintering, i.e. a powdery layer, and at a value of 0.22 are taken from fig. 6. The critical sticking velocity for the powdery layer is 0.3 m/s, which is 7.5 times larger than that of a sintered layer and 50 times larger than that of a solid plate, i.e. a fully sintered layer. It can be concluded from fig. 8 that the critical sticking velocity decreases dramatically with the degree of sintering.

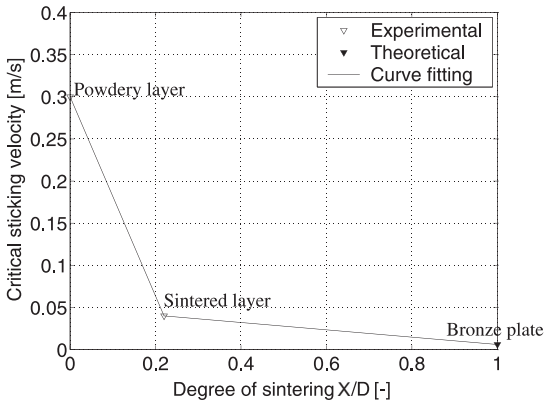

Fig. 8 The critical sticking velocity as a function of the degree of sintering X/D. Note that X is the diameter of the neck formed between the sintered particles and D is the diameter of the particles before sintering. The diameter of the bronze particles before sintering is 54 μm ± 3 μm.

The critical removal velocity (CRV) is defined as the minimum impact speed at which an incident particle can remove a particle from a bed of particles. The critical removal velocity for the layers presented in fig. 8 are given in table 2 as was determined experimentally from the impaction experiments. The critical removal velocity for the powdery layer is 0.6 m/s and for the sintered layer is larger than 3.5 m/s, which indicates that the CRV increases with sintering. Sintering strengthens the adhesion force between the particles of a particulate layer through necking, which reduces the ability of an incident particle to remove particles from the layer. Therefore, the removal rate of particles from particulate fouling layers during operation of heat exchangers will decrease as sintering starts due to the increase in the critical removal velocity.

Table 2. The critical removal velocity for the sintered layers presented in fig. 8.

Fouling layer	Degree of sintering, X/D	Critical removal velocity for the fouling layer
Powdery	0	0.6 m/s
Sintered	0.22	> 3.5 m/s
Fully sintered	1	Not defined

However, in order to model the growth rate of sintered fouling layers we should look to the removal of particles from the sintered layer itself and to the removal of the new particles deposited on the sintered layer. The critical removal velocities for a single powdery layer of bronze particles on a non-sintered bronze layer (powdery layer) and on a fully sintered bronze layer (solid plate) are presented in table 3 together with the critical removal velocity for the fouling layer itself. The critical removal velocity for a single layer of deposited particles on a fully sintered layer is calculated by the numerical model developed by Abd-Elhady et al. (2004).

The critical sticking velocity for the powdery and fully sintered layer is also presented in table 3. The critical removal velocity for a single layer of deposited particles on a fully sintered layer is 0.075 m/s, which is much smaller than the critical removal velocity for a powdery layer, 0.6 m/s. This indicates that sintering of a fouling layer reduces the CRV of the newly deposited layers, which consequently will increase the removal rate of the newly deposited particles. The change in the fouling layer microstructure from powdery to sintered decreases the deposition rate of particles and increases the removal rate of newly deposited particles, which will result in a reduction in the fouling rate as shown in fig. 1.

Table 3. The critical velocities for a powdery and a fully sintered bronze layers. The bronze particles are of average diameter 54 μm.

Fouling layer	Powdery	Fully sintered layer	Ratio= Powdery / Sintered
*Degree of sintering, X/D	0	1	0
Critical sticking velocity	0.3 m/s	0.006 m/s	50
Critical removal velocity for the fouling layer	0.6 m/s	Not defined	Not defined
Critical removal velocity for a single powdery layer on the fouling layer	0.6 m/s	0.075 m/s	8

*X is the diameter of the neck between the sintered particle and D is the diameter of the particles.

Table 3 shows the extreme conditions of particulate fouling, starting with a powdery layer and ending with a fully sintered layer. A partially sintered layer has intermediate values between the powdery and the fully sintered case as given in table 2. Once sintering has taken place due to the increase in surface temperature of the fouling layer, sintering will continue and it will never revert again to the powdery case, and the degree of sintering will increase as the sintered layer becomes thicker. Therefore, both the critical sticking and removal velocities will continue to decrease with the fouling process and sintering, such that the growth rate of the fouling layer becomes as slow as the formation of a single layer on a bare tube, which is known as the initiation period, see fig. 1. When the initiation period is longer than the characteristic sintering time (Tsantilis et al., 2001), the formed single layer become sintered and we revert again to the sintered case. In this way the asymptotic behaviour can possibly be explained.

Till so far the experiments were performed where an incident particle hits a fouling layer perpendicularly and for equally sized bed of particles. Varying both the impingement angle and the particle size distribution of the particles of the bed is relevant for analysing industrial fouling problems.

CONCLUSIONS

As the fouling layer builds up, its thermal resistance increases and therefore the temperature of the outer surface of the fouling layer increases. When the surface temperature exceeds the minimum sintering temperature of the deposits, sintering of the outer surface occurs. A sintered fouling layer lowers significantly the ability for an incident particle to stick on the fouling layer or to remove particles out of the fouling layer. However, particles that are still able to deposit on the sintered fouling layer will not sinter immediately and can therefore be removed, due to an incident particle impact. Sintering reduces the fouling rate of heat exchangers by lowering the deposition rate of new particles and increasing the removal rate of newly deposited particles such that the fouling process becomes very slow as the formation of a single layer on a bare tube, i.e. the initiation period. When the initiation period is longer than the characteristic sintering time, the formed single layer becomes sintered and we revert again to the sintered case, which leads to a very slow fouling process known as the asymptotic behaviour of particulate fouling.

NOMENCLATURE

CRS	critical sticking velocity
CRV	critical removal velocity
D	particle diameter, m
E	Young's modulus, N/m^2
e_n	coefficient of normal restitution, dimensionless
k	thermal conductivity of the fouling layer, W/mK
m	mass of particle, kg
Q_A	adhesive energy between an incident particle and a substrate during approach, J
Q'_A	adhesive energy between an incident particle and a substrate during restitution, J
Q_e	stored elastic energy in an incident particle during impact with a substrate, J
Q_p	energy loss due to plastic deformation, J
R_f	the thermal resistance of the fouling layer, m^2 K/W
SEM	scanning electron microscope
$V_{i,n}$	normal incident speed, m/s
$V_{r,n}$	normal rebound speed, m/s
X	neck diameter, m
Y	yield strength, N/m^2
δ	thickness of the fouling layer, m
ρ	density, kg/m^3
Γ	surface energy, dimensionless
ν	Poisson's ratio, dimensionless

Subscripts

i	incident
n	normal

r rebound

REFERENCES

Abd-Elhady, M. S., Rindt, C. C. M., Wijers, J. G., and van Steenhoven, A. A., 2005, Particulate fouling in waste incinerators as influenced by the critical sticking velocity and layer porosity, *Energy*, Vol. 30 (8), pp. 1469-1479.

Abd-Elhady, M. S., 2005, Gas-side particulate fouling in biomass gasifiers, *PhD thesis*, Eindhoven University of Technology, The Netherlands.

Abd-Elhady, M. S., Rindt, C. C. M., Wijers, J. G., and van Steenhoven, A. A., 2004, Removal of particles from a powdery fouled surface due to impaction, *in 2003 ECI Conference on Heat Exchanger Fouling and Cleaning: Fundamentals and Applications*; Editors: P. Watkinson, H. Müller-Steinhagen and M. Reza Malayeri, Santa Fe, New Mexico, United States, pp. 128-136, Berkly Electronic Press.

Baxter, L. L., 1993, Ash deposition during biomass and coal combustion: a mechanistic approach, *Biomass and Bioenergy*, Vol. 4, no. 2, pp. 85-102.

Bott, T. R., 1988, Gas side fouling, *Fouling Science and Technology*, pp. 191-203.

Brunner, T., Joeller, M., Obernberger, I., and Frandsen, F., 2002, Aerosol and fly ash formation in fixed bed biomass combustion systems using woody biofuels, *Proceedings of the 12st European Conference on Biomass for Energy, Industry and Climate protection 2002*, Amsterdam, The Netherlands, pp. 685- 689.

Bryers, R. W., 1996, Fireside slagging, fouling and high-Temperature corrosion on heat-transfer surface due to impurities in steam-raising fuels, *Progress in Energy and Combustion Science*, Vol. 22, pp. 29-120.

Cleaver, J. W. and Yates, B., 1975, A sub layer model for the deposition of particles from a turbulent flow, *Chemical Engineering Science*, Vol. 30, pp. 983-992.

Fan, F. G., and Ahmadi, G., 1993, A sub layer model for turbulent deposition of particles in vertical ducts with smooth and rough surfaces, *Journal of Aerosol Science*, Vol. 24, pp. 45-64.

Frenkel, J., 1945, Viscous flow of crystalline bodies under the action of surface tension, *Journal of Physics (Moscow)*, Vol. 9, pp. 385-391.

Friedlander, S. K., and Johnstone, H. H., 1957, Deposition of suspended particles from turbulent gas streams, *Industrial and Engineering Chemistry*, Vol. 49, pp. 1151-1156.

Israel, R., and Rosner, D. E., 1983, Use of a generalized Stokes number to determining the aerodynamic capture efficiency of non-Stokesian particles from a compressible gas flow, *Aerosol Science and Technology*, Vol. 2, pp. 45-51.

Johnson, K. L., 1985, *Contact Mechanics*, Cambridge University press.

Kern, D. Q., and Seaton, R. E., 1959, A theoretical analysis of thermal surface fouling, *Chemical Engineering Progress*, Vol. 4, pp. 258-262.

Kuczynski, G. C., 1949, Self-diffusion in sintering of metallic particles, *Trans. AIME*, vol. 185, pp. 169-178.

Miles, T. R., Baxter, L. L., Bryers, R. W., Jenkins, B. M., and Oden, L. L., 1996, Boiler deposits from firing biomass fuels, *Biomass and Bioenergy*, Vol. 10, pp. 125-138.

Papavergos, P. G., and Hadley, A. B., 1984, Particle deposition behaviour from turbulent flows, *Chemical Engineering Research and Design*, Vol. 62, pp. 275-295.

Ristic, M. M., 1979, *Sintering-New Developments*, Elsevier Scientific Publisher Company, Amsterdam.

Rogers, D. E., and Reed, J., 1984, The adhesion of particles undergoing an elastic-plastic impact with a surface, *Journal of Physics D: Applied Physics*, Vol. 17, pp. 677-689.

Rosner, D. E., 1980, Thermal (Soret) diffusion effects on interfacial mass transport rates, *PhysicoChemical Hydrodynamics*, Vol. 1, pp. 159-185.

Thornton, C., and Ning, Z., 1998, A theoretical model for the stick/bounce behaviour of adhesive, elastic-plastic spheres, *Powder Technology*, Vol. 99, pp. 154-162.

Tsantilis, S., Briesen, H. and Pratsinis, S. E., 2001, Sintering time for silica particle growth, *Aerosol Science and Technology*, Vol. 34(3), pp. 237-246.

Van Beek, M. C., Rindt, C. C. M., Wijers, J. G., and van Steenhoven, A. A., 2001, Analysis of fouling in refuse waste incinerators, *Heat Transfer Engineering*, Vol. 22, pp. 22-31.

Van Beek, M. C., 2001, Gas-Side Fouling in Heat-Recovery Boilers, *PhD thesis*, Eindhoven University of Technology, The Netherlands.

Wagoner, C. L., and Yan, X-X., 1991, Deposit initiation via thermophoresis: Part 1. Insight on deceleration and retention of inertially transported particles, *Inorganic Transformations and Ash Deposition during Combustion*, ed. S.A. Benson, ASME New York, pp. 607-624.

Wall, T. F., Bhattacharya, S. P., Zhang, D. K., Gupta, R. P., and He, X., 1993, The properties and thermal effects of Ash deposits in coal-fired furnaces, *Progress Energy Combustion Science*, Vol. 19, pp. 487-504.

Wood, N. B., 1981, A simple method for the calculation of turbulent deposition to smooth and rough surfaces, *Journal of Aerosol Science*, Vol. 12, pp. 275-290.